

Oliver Montenbruck
Miquel Garcia-Fernandez
Jacob Williams

Performance comparison of semicodeless GPS receivers for LEO satellites

Received: 4 November 2005
Published online: 22 March 2006
© Springer-Verlag 2006

O. Montenbruck (✉)
Miquel Garcia-Fernandez
German Space Operations Center,
Deutsches Zentrum für Luft- und
Raumfahrt, 82230 Weßling,
Germany
E-mail: oliver.montenbruck@dlr.de
Tel.: +49-8153-281195
Fax: +49-8153-281450

J. Williams
Center for Space Research,
University of Texas at Austin,
Austin, TX 78759, USA

Abstract This report provides a detailed performance analysis of three semicodeless dual-frequency GPS receivers for use in low Earth orbit (LEO). The test set comprises the IGOR receiver, which represents a follow-on of the flight-proven BlackJack receiver, as well as two geodetic receivers (NovAtel OEM4-G2 and Septentrio PolaRx2), which are entirely based on commercial-off-the-shelf technology (COTS). All three receivers are considered for upcoming flight projects or experiments and have undergone at least a preliminary environmental qualification program. Using extensive signal simulator tests, the cold start signal acquisition, tracking sensitivity, differential code biases, raw measurement accuracy, and navigation accuracy of each receiver have been assessed. All tests are based on a common scenario that is representative of an actual space mission

and provides a realistic simulation of the signal dynamics and quality on a scientific LEO satellite. Compared to the other receivers, the IGOR instrument exhibits a superior tracking sensitivity and is thus best suited for occultation measurements with low tangent point altitudes. The OEM4-G2 and PolaRx2 receivers are likewise shown to properly track dual-frequency GPS signals and normal signal levels and to provide accurate code and carrier phase measurements. Given their limited resource requirements, these receivers appear well suited for precise orbit determination applications and ionospheric sounding onboard of microsatellites with tight mission budgets.

Keywords Spaceborne GPS · Semicodeless tracking · IGOR · OEM4-G2 · PolaRx2 · BlackJack

Introduction

Similar to terrestrial applications, dual-frequency GPS receivers offer numerous advantages over single-frequency receivers in space applications. Even though the basic navigation requirements of many spacecraft can well be met by single-frequency receivers, the second frequency is of great interest for scientific missions and a key to ultimate accuracy in absolute and relative navigation (Yunck 2004). It allows the direct elimination of ionospheric path delays and thus gives full access to the

accuracy of carrier-phase based measurements. GPS tracking of low Earth satellites has dramatically improved our knowledge of the Earth's gravity field (Reigber et al. 2004) and GPS based radio occultation measurements are an indispensable source of information for ionospheric and tropospheric research (Kursinski et al. 1997). In carrier-phase differential GPS (CDGPS), dual-frequency measurements enable a reliable resolution of integer ambiguities even at large baselines and non-negligible differential ionospheric delays (Kroes et al. 2005).

Over the past decade, scientific applications of spaceborne GPS have almost exclusively relied on the BlackJack (or TurboRogue Space Receiver, TRSR-2) receiver. This receiver has been developed by NASA's Jet Propulsion Laboratory (JPL) and successfully flown on numerous satellites including Oersted, Champ, SAC-C, ICESat, GRACE, and Jason-1. More recently, JPL has licensed core technology to Broadreach Engineering, which now manufactures the IGOR receiver as a BlackJack follow-on version with improved space hardness. Within Europe, ESA has continuously supported and promoted the independent development of dual-frequency receivers for space applications through the AGGA (Advanced GPS/GLONASS ASIC) correlator. These efforts have resulted in the GRAS instrument of SAAB Aerospace to be flown onboard the METOP satellite as well as Laben's Lagrange receiver, which, for example, has been selected for ESA's GOCE mission.

All of the aforementioned receivers are characterized by a high level of specialization, a limited production volume, and a demanding qualification program. This results in a representative price tag of \$1 million and bursts the budget of typical small satellite science missions. In view of this situation, scientists and industry have repeatedly expressed their interest in affordable alternatives for missions where utmost reliability and rigorous space qualification may not be mandatory. Based on promising experience with single-frequency receivers, DLR has therefore taken the initiative to investigate the use of existing commercial-off-the-shelf (COTS) dual-frequency receivers for space applications and to perform a basic qualification program as well as initial flight demonstrations. As part of this effort, NovAtel's OEM4-G2L and Septentrio's PolaRx2 receiver have been demonstrated to cope with the signal dynamics and the environmental conditions of a low Earth satellite (Langley et al. 2004; Leyssens and Markgraf 2005). Further motivation for the adaptation of COTS receivers stems from the fact that the BlackJack receiver has itself evolved from prior generations of digital receivers for high-precision ground use (Rogue, TurboRogue).

The present study provides a detailed performance assessment and comparison of the space qualified IGOR receiver with the COTS-based OEM4-G2 and PolarRx2 receivers (cf. Fig. 1) based on a harmonized set of signal simulator tests. Key parameters of the three employed receivers are summarized in Table 1. Following a general characterization of each receiver, the simulator test scenario and the fundamental analysis steps are described in the subsequent sections of this report. Aside from the basic questions of tracking and navigation accuracy, the study addresses the cold start time, the tracking sensitivity, semicodeless tracking losses, and differential code biases (DCBs) to enable a proper characterization of the receiver performance.

For completeness, we mention that at least three other semicodeless dual-frequency GPS receivers for space applications are currently offered by European and Japanese manufacturers but could not be accessed for the present study. These include the Lagrange receiver of Laben (Marradi et al. 2001), the GRAS instrument of SAAB Aerospace (Silvestrin et al. 2000), and the dual frequency space receiver (DFSG) of NEC/Toshiba (Buist 2002). So far, however, no relevant laboratory test data or in-flight performance data have been publicly released for any of these receivers. The test strategy described in this report may nevertheless provide a guideline for future analysis and serve as a basis for an extended comparison of spaceborne GPS receivers.

Receivers

IGOR

The IGOR Integrated GPS and Occultation Receiver (BRE 2003) is a follow-on of JPL's BlackJack GPS receiver for space applications. IGOR closely matches the CHAMP BlackJack design but employs a higher degree of space qualified electronics components than JPL's original version. First flights of the IGOR receiver are foreseen in 2005/2006 onboard the Taiwanese Formosat-3 (formerly COSMIC) constellation (Wu et al. 2005) and the German TerraSAR-X mission.

The receiver supports a total of four antenna inputs, which can be flexibly assigned for navigation and occultation measurements. The 48 individual receiver channels can be allocated in sets of three to track C/A-, P1-, and P2-code for up to 16 GPS satellites. During anti-spoofing, a patented, codeless tracking technique is used to estimate P-code from the encrypted Y-code (Thomas 1995; Meehan et al. 2000). Aside from the main tracking mode, the receiver can operate in occultation mode to collect measurements when GPS satellites rise or set. Even though the original design of the BlackJack receiver involves a large number of COTS components, extensive ground tests and the available flight experience provide adequate evidence for its survivability in a space environment. The IGOR receiver is specified to tolerate a total ionization dose of at least 12 krad (Table 1), which is adequate for mission durations of several years in a low Earth orbit (LEO). A high level of fault tolerance is provided through four independent R/F input strings and two independent digital sections.

Due to its use in multiple space missions the BlackJack receiver is well characterized by laboratory tests and in-flight validations (Williams et al. 2002; Montenbruck and Kroes 2003) and similar results may be expected for the IGOR design. For the present tests, the TerraSAR-X flight unit has been made available by the GeoForschungsZentrum (GFZ), Potsdam and the

Fig. 1 Test receivers: IGOR, NovAtel OEM4-G2, and Septentrio PolaRx2 (left to right; note different scales)

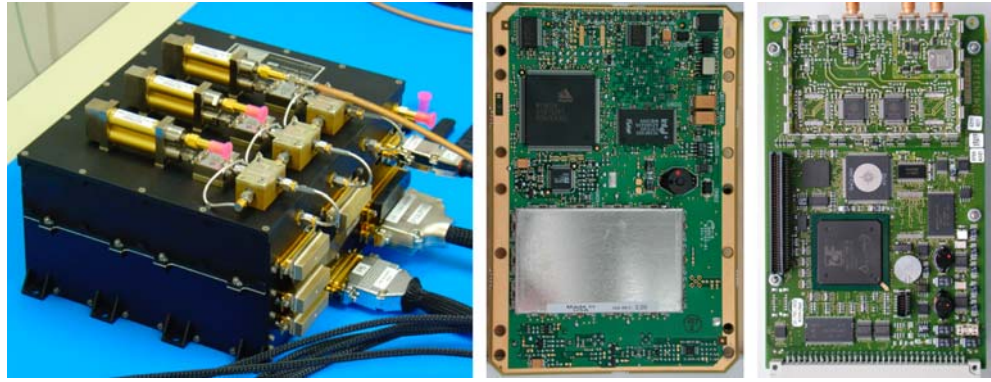


Table 1 Test receivers characteristics. Measurement types are specified by the respective Rinex 2.20 designators (see Gurtner and Estey 2002). Size, mass, and power consumption for the OEM4-G2 and PolaRx2 receivers refer to the standalone receiver board without peripheral electronics and housing

Parameter	IGOR	OEM4-G2 (OEM4-G2L)	PolaRx2 (PolaRx2@)
Manufacturer	Broadreach Engineering (Jet Propulsion Laboratory)	NovAtel	Septentrio
Country of Origin	USA	Canada	Belgium
Type	Receiver with support electronics and housing	Receiver board	Receiver board
Signals	GPS L1/L2	GPS L1/L2	GPS L1/L2, SBAS L1
Antenna Inputs	4	1	1 (3)
Channels	3×16	2×12	3×16
Measurement types	C1, P1, P2, LA, L1, L2, SA, S1, S2	C1, P2, LA, L2, SA, S2	C1, P1, P2, LA, L2, DA, D2, SA, S1, S2
Size	$200 \times 240 \times 110 \text{ mm}^3$	$85 \times 125 \times 20 \text{ mm}^3$ ($60 \times 100 \times 15 \text{ mm}^3$)	$180 \times 100 \times 15 \text{ mm}^3$
Mass	4.6 kg	85 g (60 g)	190 g
Power	16 W	2.5 W (1.5 W)	5 W (7 W)
Operating temperature	-10 to +55°C	-15 to +55°C	-30 to +45°C
Total ionization dose	12 krad	6 krad	9 krad
Missions	COSMIC (2005), TerraSAR-X (2006)	CASSIOPE (2007), CanX-2 (2006)	TET108 (2008)

TerraSAR-X project. It differs from the standard IGOR design through the use of external low noise amplifiers and additional band-pass filters at the R/F input.

OEM4-G2

NovAtel's OEM4-G2 is a dual-frequency COTS receiver originally designed for terrestrial and aeronautical applications. It employs a MINOS-4 correlator and offers a total of 2×12 tracking channels for C/A-code tracking on the L_1 frequency and P-code tracking on L_2 . In case of anti-spoofing a proprietary semi-codeless technique is used to obtain P2 measurements from the encrypted Y-code without explicit knowledge of the encryption code (Fenton 1998). Since the

OEM4-G2 does not explicitly track P(Y)-code on L_1 , care must be taken to properly account for receiver and transmitter induced DCBs when working with an ionosphere-free combination of C1 and P2 pseudoranges.

Besides the standard OEM4-G2 receiver, NovAtel has introduced the OEM4-G2L receiver which offers a higher integration and lower power consumption but otherwise employs the same correlator and tracking software. The small form factor, weight, and power requirements make the OEM4-G2 and OEM4-G2L receivers of particular interest for microsatellite missions with intrinsically tight onboard resources. As part of the environmental qualification program, the OEM4-G2L receiver has been shown to survive a total ionization dose of approximately 6 krad without further hardware

modifications (Markgraf and Montenbruck 2004). While this is considered adequate for LEO mission durations of up to 2 years, further investigations of the single-event upset and latch-up sensitivity of the receiver are presently pending.

In view of promising test results and the modest hardware cost, the OEM4-G2L receiver has been selected for the e-POP payload of the Canadian CAScade Demonstrator Smallsat and Ionospheric Polar Explorer (CASSIOPE) mission (Langley et al. 2004). Launch of the spacecraft is presently scheduled for 2007 and will provide complementary flight experience for the use of COTS based dual frequency GPS technology in space. Even 1 year earlier, an experimental flight of an OEM4-G2L receiver is planned onboard the CanX-2 picosatellite of the University of Calgary (Rankin 2004).

PolaRx2

As a spin-off from ESA's AGGA correlator development, the Belgian company Septentrio has developed the GNSS Receiver Core (GreCo) and a matching front-end chip (GreFe) for use in geodetic dual-frequency GPS receivers. Their recent PolaRx2 receiver offers a total of 48 channels for GPS and SBAS tracking and is available in versions with one or three antenna inputs. Three individual channels are normally combined to perform C/A-code and P(Y)-code tracking on the L_1 and L_2 frequency of a single GPS satellite. The semicodeless tracking concept employed with the family of AGGA and GreCo correlators (Silvestrin and Cooper 2000) resembles the well-known Z-tracking scheme (see, e.g. Woo 2000) for encrypted P-code but is expected to provide a better estimation of the W-code bit and thus a reduction of the implied squaring losses. The use of tight correlator spacings and narrow tracking loop bandwidths furthermore contributes to high-quality code and carrier.

As part of a qualification program for in-orbit applications conducted by DLR and Septentrio (Leysens and Markgraf 2005), the PolaRx2 receiver has undergone a first series of signal simulator and environmental tests (total ionization dose, thermal/vacuum, and vibration). In this context, the PolaRx2 firmware has received minor modifications and patches to properly support the signal dynamics encountered onboard a LEO satellite. The Doppler search window has been extended to 45 kHz to ensure a robust cold start acquisition, but no changes of the tracking loop parameters were performed. For use in space environment, the PolaRx2 receiver has demonstrated an adequate range of operations temperatures and total dose resistance (9 krad) but presently lacks a characterization of single-event upset and latch-up sensitivity as well as dedicated protective measures. Within DLR's On-Orbit

Verification program a demonstration flight of the PolaRx2 receiver is presently foreseen onboard the TET108 satellite in 2008.

Performance testing and analysis

Test configuration

The tests employed for the present performance study have been conducted on Spirent STR4760 and STR7790 GPS signal simulators (Spirent 2004), which allow for a realistic modeling of a spaceborne user trajectory. A sun-synchronous, polar orbit with an altitude of 515 km and an inclination of 97.44° has been adopted, which closely resembles the TerraSAR-X mission profiles. The modeling of ionospheric path delays has been based on the assumption of a constant vertical total electron content of 10 TECU and a Lear mapping function (Lear 1987). In accord with the study scope, no broadcast ephemeris errors, clock dithering, or multipath errors have been applied in the simulations. Based on the specified GPS constellation data and the simulated user satellite trajectory, truth values of the pseudoranges for each observed GPS satellite have been computed offline for comparison with the actual receiver measurements.

For a realistic simulation of observed signal strengths, we adopted the gain pattern of a Sensor Systems S67-1575-14 GPS antenna with choke ring, which is currently employed on various satellites such as CHAMP and GRACE. A digitized antenna diagram for use with Spirent signal simulators has been generated within the ICESat project (Williams et al. 2002) and made available for the present analysis. Based on reference data from outdoor tests, the power of the L_1 C/A code signal generated by the simulator was adjusted such as to achieve a closely matching range of C/N_0 readings in the simulations.

As noted by Van Dierendonck (1995), a higher than normal signal level is usually required to compensate for the higher noise temperature experienced in simulator testing compared to the usual antenna sky temperature. While an increase of about +8 to +10 dB has earlier been recommended for single-frequency receivers with narrow front-end band widths in Montenbruck and Holt (2002), notably higher signal levels were required for the employed dual-frequency receivers. Even though all test receivers were operated with external low noise amplifiers designed for use with a passive antenna, the signal level at the R/F outlet of the simulator had to be raised by +13 to +17 dB relative to a nominal L_1 C/A code signal power of -130 dBm. In accord with the GPS signal specification the P-code signal power was furthermore configured to be 3 dB less than that of the C/A code signal on the L_1 frequency and 6 dB less on the L_2 frequency.

Finally, the antispoofting bit (i.e. bit 19 of the hand-over word) was activated in the navigation messages to ensure that none of the test receivers would attempt a direct P-code acquisition. Even though the Spirent simulators also provide for the generation of a pseudo-Y-code (or Z-code), use of this feature did not affect the tracking accuracy in our tests.

Cold start acquisition

As a prerequisite for operation in a LEO, a spaceborne GPS receiver must be able to properly acquire GPS signals and to compute an initial navigation solution irrespective of the involved signal dynamics. Due to the high orbital velocity of a LEO satellite, a maximum range rate of ± 8.5 km/s can be encountered near rising or setting of a GPS satellite. Along with uncertainties of the local reference frequency, the receiver must thus accommodate a typical Doppler search space of ± 45 kHz for a guaranteed cold start acquisition. While various single-frequency GPS receivers for space applications support a warm start acquisition based on a priori time and orbit information, no such features are available in any of the receivers considered here. On the other hand, the IGOR, OEM4-G2, and PolRx2 receivers benefit from a large number of individual correlator channels which enable a parallel search of code/frequency bins and a corresponding reduction of the acquisition time.

To assess the cold start performance, a series of receiver reboots has been conducted at random epochs throughout the simulated test scenario. All receivers were able to safely acquire satellites and to achieve navigation fix in due time, but notable performance differences were obvious (cf. Table 2). Surprisingly, the IGOR receiver exhibited the longest time-to-first-fix (TTFF) despite its dedicated design for space use and an adequately large number of tracking channels. After power-up, the receiver remains in a start-up state (beep mode) for about 2 min before the actual signal search is initiated. Thereafter it took between 3 and 14 min to achieve a first navigation fix. The average TTFF amounted to roughly 10 min (including beep mode).

Among the three receivers considered here, the OEM4-G2 appears least prepared for GPS signal acquisition in LEO due to the moderate number of correlator channels and the restricted Doppler search

window of ± 4.5 kHz. However, most of the time, there exists a subset of visible GPS satellites for which the Doppler shift is within the reduced search range of terrestrial receivers. This results in adequate acquisition times even for unmodified receivers such as the OEM4-G2. After power-up, the receiver took about 7 s to start operation and mostly locked to the C/A code of a first GPS satellite just a few seconds later. Following a successful frame lock and decoding of the frame header, a coarse time was generally available within about 40 s after boot. A navigation fix (requiring four tracked satellites and successful decoding of the respective navigation messages) was achieved within 2–10 min. Once the position and velocity were known to the receiver, the remaining satellites were acquired within less than a minute, if a valid almanac was available in the nonvolatile memory (NVM). Otherwise, the acquisition of the full GPS constellation could take at most 12.5 more minutes.

The best overall results were achieved by the PolRx2 receiver which obtained a full navigation fix within 1–3 min after a reboot in cold start conditions. This performance may in part be attributed to the large number of correlator channels and an adequate Doppler search space, even though the same is obviously true for the IGOR receiver as well. From an operational point of view, the short acquisition time is of great benefit and may serve as a reference for the design of future space receivers. It helps to minimize the outage times after occasional receiver set-ups and allows a power-saving, intermittent receiver utilization.

Signal-to-noise ratio and squaring losses

For a given tracking loop design, the achieved code and carrier noise in a GPS receiver is primarily a function of the signal quality as measured by the ratio C/N_0 of carrier to noise power in a 1 Hz bandwidth. As a reference for the proper interpretation of data provided later in this report we first determined the variation of C/N_0 with elevation in a series of outdoor tests (Ardaens 2005). The employed antenna system comprises a passive Sensor Systems S67-1575-14 antenna with choke ring and a Spectrum Microwave preamplifier with a noise figure of better than 2 dB. For the IGOR receiver, no such tests could be conducted, but flight data of the CHAMP BlackJack receiver were available as a substitute. Following Montenbruck and Kroes (2003) the relation

$$\frac{C}{N_0} = 20 \log_{10} \left(\frac{\text{SNR}}{\sqrt{2}} \right). \quad (1)$$

was employed to convert the signal-to-noise amplitude ratios (SNR in units of V/V) given by the BlackJack and

Table 2 Cold start acquisition times

Receiver	TTFF	Notes
IGOR	3–16 min	Including 2 min “beep mode”
OEM4-G2	2–10 min	
PolRx2	1–3 min	Including initial self-test

IGOR receivers to the more common carrier-to-noise-density ratio (in dB-Hz).

As shown in Fig. 2, C/N_0 values of 51 and 53 dB-Hz near zenith can be achieved with the OEM4-G2 and PolaRx2 receivers for the L₁ C/A code signal. For lower elevations almost identical results are obtained with both receivers. The BlackJack (IGOR) results, on the other hand, are systematically higher by about 3 dB and exhibit a peak value of 55 dB-Hz. All receivers tracked GPS satellites down to the horizon where the antenna gain is roughly 17 dB lower than in the boresight direction. Below 20° elevation multipath induced signal strength variations are evident in the terrestrial data, while the CHAMP onboard environment is virtually free of reflected signal.

The three receivers considered in our test employ their own proprietary semicodeless tracking schemes to obtain P-code measurements during antispoofing. These are based on public knowledge of the P-code sequence and the assumption that the encrypted Y-code results from P-code by multiplication with an unknown W-code at a frequency of roughly 500 kHz. To estimate the unknown W-code chip sequence, all semicodeless tracking schemes involve signal multiplications that result in a decrease of the signal-to-noise ratio compared to a direct carrier tracking. As shown in the overview of Woo (2000), the magnitude of the associated squaring losses depends on the particular tracking scheme, but is proportional to the carrier-to-noise density itself for medium and low C/N_0 values. With modern receivers a squaring loss of -7 to -10 dB

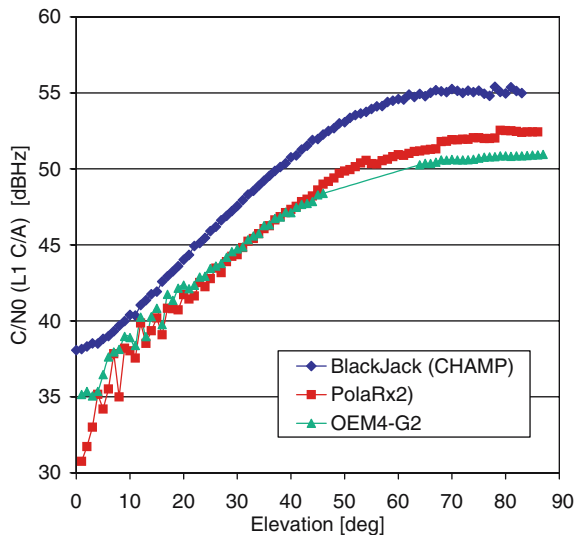


Fig. 2 Carrier-to-noise-density ratios for L₁ C/A code as obtained with the BlackJack receiver onboard the CHAMP satellite and in ground tests with the OEM4-G2 and PolaRx2 receivers. All data have been collected with identical antennas (Sensor Systems S67-1575-14) and choke rings

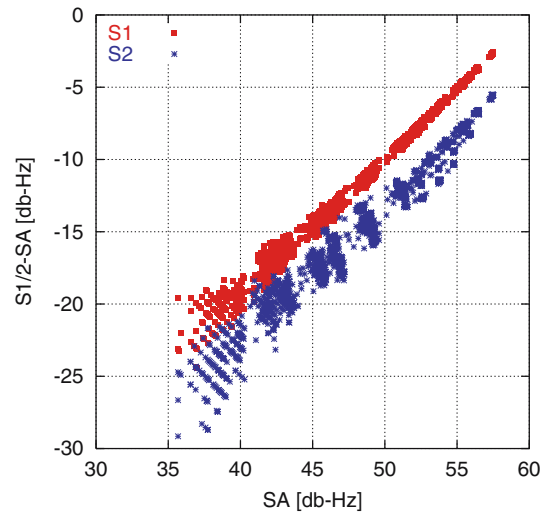


Fig. 3 Semicodeless tracking losses of the IGOR receiver as illustrated by the difference between the measured C/N_0 for P-code tracking (S1, S2) and C/A code tracking (SA). The applied signal strengths for P-code on L₁ and L₂ were 3 and 6 dB lower than those for C/A code on L₁

is obtained at an L₂ C/N_0 of 45 dB-Hz, but increases to -16 to -19 dB at 35 dB-Hz.

As a measure of the semicodeless tracking quality, most dual-frequency receivers provide signal-to-noise ratios (RINEX data type S1 and S2) for P(Y)-code tracking on L₁ and L₂ in addition to their estimate of the L₁ C/N_0 ratio (SA). For comparing the squaring losses of semicodeless tracking in the three test receivers, the size of the S1-SA difference and/or S2-SA difference is shown in Figs. 3, 4, and 5 as a function of SA. The respective measurements have been collected in the simulator test bed using the relative signal strength settings specified above and do not account for differences in the L₁ and L₂ antenna gain patterns. For both the IGOR and PolaRx2 receivers, S1 and S2 provide signal-to-noise ratios *including* the squaring losses such that the S1-SA and S2-SA differences exhibit the expected linear variation with SA over the full range of observed signal strengths. Within the limitations imposed by the observed scatter of S1 and S2 measurements, an essentially equal performance of semicodeless tracking schemes in the PolaRx2 and IGOR receivers may be inferred. It is further noted that the S2 values are almost identical to S1 in the PolaRx2 receiver, which suggest that S2 is not fully representative of the P-code signal strength on L₂.

S2 measurements provided by the OEM4-G2 exhibit a notably different variation with SA and cannot be interpreted in the same way as those of the other receivers. The difference of S2 and SA varies between -5 and -10 dB and it may be speculated whether the receiver attempts to recover the true carrier-to-noise density ratio for L₂ P-code. In any case no assessment of the

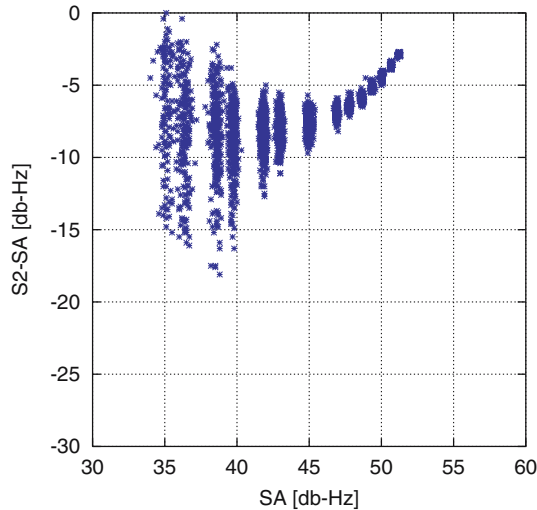


Fig. 4 Difference between the measured carrier-to-noise density for P-code tracking (S2) and C/A code tracking (SA) for the OEM4-G2 receiver

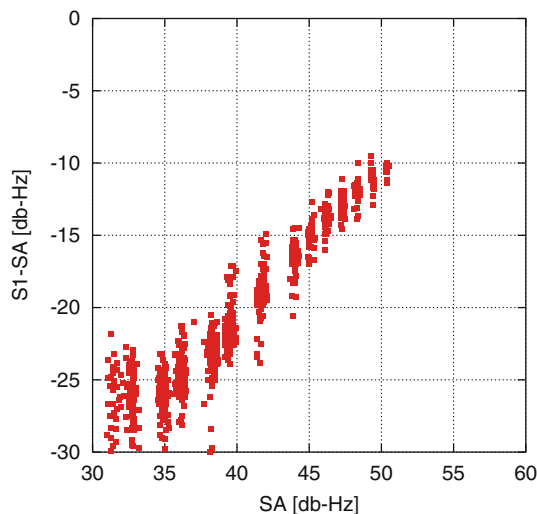


Fig. 5 Difference between the measured carrier-to-noise density for P-code tracking (S1) and C/A code tracking (SA) for the PolaRx2 receiver. S2 results are almost identical and have been omitted for clarity

semicodeless tracking losses can be obtained from the S2 measurements for this particular receiver.

Code- and carrier phase noise analysis

The raw measurement quality of the IGOR, OEM4-G2, and PolaRx2 receivers has been assessed based on three distinct strategies:

1. A “virtual” zero baseline test (vZB) analyzing double differences of code- and carrier phase measurements from consecutive signal simulator runs to determine the noise properties.
2. The multipath (MP) combination to determine the code noise characteristics without a need for differencing across multiple receiver data.
3. A comparison of single difference code- and carrier phase measurements with simulator truth values to determine systematic measurement errors (that are cancelled in the zero-baseline test).

All concepts are designed to require only a single receiver unit, which is particularly useful in view of the high cost and limited availability of spaceborne GPS receivers.

In a traditional zero-baseline test, double differences ($\nabla\Delta$) of code and phase measurements ρ from two receivers and two commonly observed GPS satellites are formed. For receivers connected to the same signal source, the result no longer depends on the geometric distance, clock errors, and atmospheric path delays, but only on the receiver internal measurement noise ε . By selecting satellite pairs with closely matching C/N_0 (typically less than 1 dB-Hz) the noise of each individual measurement can be assumed to exhibit the same standard deviation, which is then obtained from

$$\sigma(\varepsilon) = \frac{\sigma(\nabla\Delta\rho)}{\sqrt{4}}. \quad (2)$$

When working with a properly calibrated GPS signal simulator, the zero-baseline test can alternatively be conducted with data sets collected by a single receiver in two consecutive simulator runs. Since the same models are applied in the signal generation during repeated simulations, the signals differ only by noise originating from the simulator’s internal reference frequency. This noise contribution is identical for all simulator channels and therefore cancels upon forming double differences.

To enable a proper differencing in a zero-baseline test, the employed measurements must ideally be collected at exactly the same times. Given the maximum range-rate experienced by a GPS receiver onboard a LEO satellite, the measurement epochs must be synchronized to better than 50 ns to introduce an error of less than 0.5 mm in the analysis of carrier phase double differences. Except for the OEM4-G2 receiver, which continuously steers its clock to GPS time within the limits implied by the navigation solution accuracy, this synchronization cannot, however, be achieved in practice. In the IGOR receiver, the clock offset is typically controlled within a 1 μ s deadband, while the PolaRx2 performs discrete clock adjustments between 1 ms bounds. Accordingly, all measurements collected by these receivers have been propagated to integer seconds of GPS time using measured or interpolated range rates.

It may be noted that the same type of preprocessing would also be mandatory in carrier phase differential GPS applications.

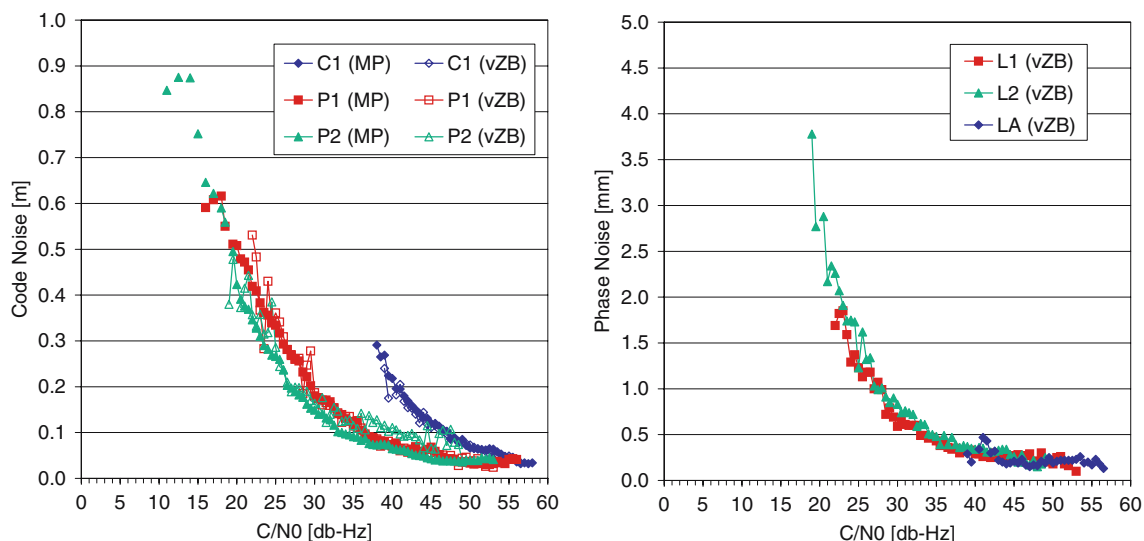
Since zero-baseline testing requires pairs of measurements with (near-)equal C/N_0 ratios, long data arcs are usually required to obtain proper statistics for the full range of observed signal strengths. As an alternative, the code noise performance can also be assessed based on code-carrier differences (see, e.g. Montenbruck and Kroes 2003). It can be used with much shorter data sets and is equally suitable for simulator testing and in-flight analyses. By forming the geometry-free and ionosphere free MP combinations

$$\begin{aligned} \rho_{CA} - \rho_{L1} - \frac{2f_2^2}{f_1^2 - f_2^2}(\rho_{L1} - \rho_{L2}) - b_{CA} &\approx M_{CA} + \varepsilon_{CA} \\ \rho_{P1} - \rho_{L1} - \frac{2f_2^2}{f_1^2 - f_2^2}(\rho_{L1} - \rho_{L2}) - b_{P1} &\approx M_{P1} + \varepsilon_{P1} \\ \rho_{P2} - \rho_{L2} - \frac{2f_1^2}{f_1^2 - f_2^2}(\rho_{L1} - \rho_{L2}) - b_{P2} &\approx M_{P2} + \varepsilon_{P2} \end{aligned} \quad (3)$$

only receiver specific code tracking errors are retained. Here f_{L1} and f_{L2} are the GPS signal frequencies. The biases b are individually adjusted for each continuous tracking pass such as to achieve a zero mean right-hand side for multipath-free, high elevation observations. Since the simulator test bed is free of unintentional multipath errors (M), only receiver noise (ε) remains, which may then be correlated with the carrier-to-noise-density reading of the receiver.

Results of the vZB and the MP combination analysis for the three test receivers are shown in Figs. 6, 7, and 8.

Fig. 6 IGOR code noise (*left*) and carrier phase noise (*right*) as a function of carrier-to-noise-density. *Individual lines* indicate results based on multipath-combination (MP) and virtual zero-baseline test (vZB)



These provide the estimated measurement noise as a function of C/N_0 in 1 dB-Hz bins for the supported data types of each receiver. Both methods yield consistent values for the C/A, P1 and P2 code noise, even though results based on the MP combination can be obtained with much shorter data sets and exhibit a notably lower scatter. For completeness, it is noted that the code noise analysis may in part be affected by correlations of consecutive measurements, even though no relevant differences have been noted in the processing of OEM4-G2 and PolaRx2 data sets at 1 and 10 s sampling intervals. In the case of IGOR receiver, the 10-s measurement samples are guaranteed to be free of correlations.

Systematic carrier phase errors

Complementary to the noise analysis described in the previous section, we have made an effort to analyze possible systematic measurement errors related to the tracking loop design or the measurement timing inside the test receivers. For this purpose, an analysis concept introduced in Montenbruck and Holt (2002) has been employed. Here single differences for two observed GPS satellites are formed to eliminate the receiver clock error. The result is subsequently differenced against truth values of the single-difference pseudoranges that have been computed consistently with the internal modeling of the signal simulator. While common receiver errors are cancelled in a regular zero-baseline test, they can be easily identified in comparison with the truth data.

The results show no indications of errors proportional to the line-of-sight acceleration (or Doppler rate of change) that would be expected in the case of second-order tracking loops. We may conclude that even the OEM4-G2 and PolaRx2 receivers employ a third-order PLL for tracking the L1 carrier, which again confirms

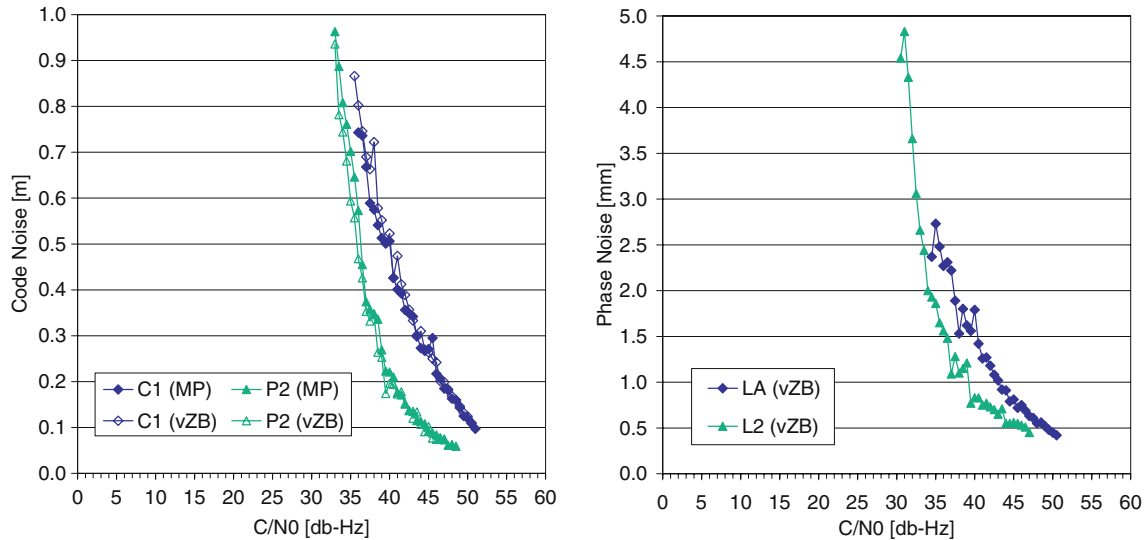


Fig. 7 OEM4-G2 code noise (*left*) and carrier phase noise (*right*) as a function of carrier-to-noise density

their ability to properly cope with the signal dynamics onboard a LEO satellite.

On the other hand, subtle errors in proportion to the range rate have been identified in the carrier phase measurements of all three receivers. These errors can readily be interpreted as receiver dependent timing offsets and removed by a correction of the respective measurement time tags. In the IGOR and PolaRx2 receiver a consistent offset applies for all types of phase observations (i.e. LA, L1, and L2), while the OEM4-G2

requires a different correction for its LA and L2 carrier phase measurements. Consistent results have been obtained with various OEM4-G2 and PolaRx2 receiver units, which suggests that the timing errors are primarily related to the hard- and software design of the respective receivers. Even though the absolute values of the time offsets given in Table 3 may in part be affected by the employed signal simulators, the variation across receiver types is conclusively determined and of key relevance in practical applications. Care must thus be taken when using mixed receiver types for relative navigation applications (e.g. rendezvous and docking or formation flying) of spacecraft in LEO. Here errors of up to several centimetres may occur in double differences of uncorrected carrier phase measurements. For common receivers, in contrast, the systematic time offsets are fully cancelled. This is nicely illustrated by the GRACE mission, where high accuracy relative naviga-

Fig. 8 PolaRx2 code noise (*left*) and carrier phase noise (*right*) as a function of carrier-to-noise density

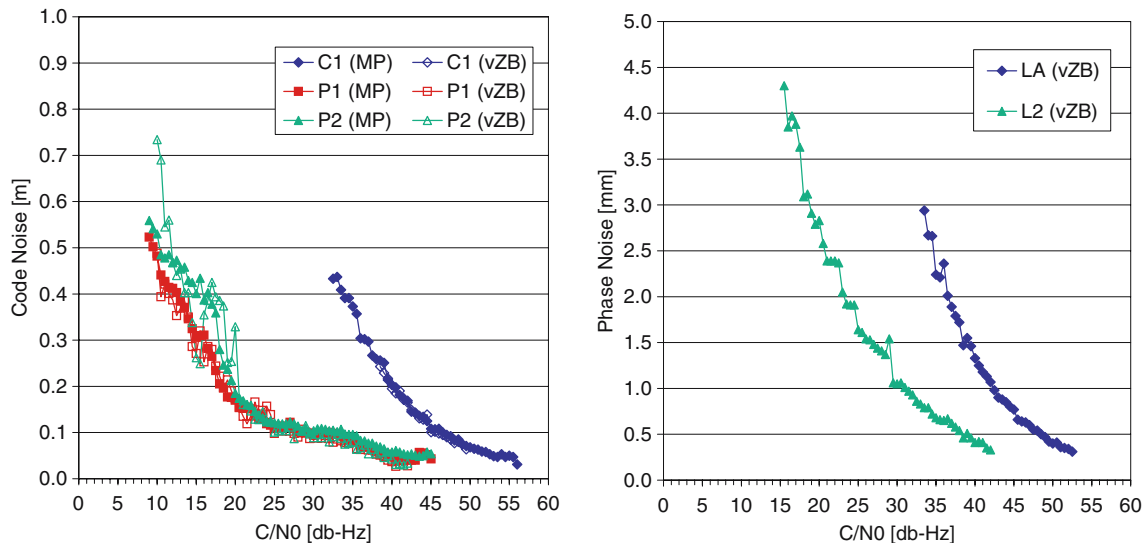


Table 3 Carrier phase time offset relative to the code-based clock solution. The specified values need to be added to the time stamp given by the receiver to obtain the true measurement epoch

Receiver	LA/L1 (μs)	L2 (μs)
IGOR	-0.45 ± 0.05	-0.45 ± 0.05
OEM4-G2	-1.00 ± 0.10	-3.10 ± 0.10
PolaRx2	-0.60 ± 0.05	-0.60 ± 0.05

tion results were obtained without any time offset correction (see Kroes et al. 2005).

Differential code biases

In search for systematic tracking errors, we have furthermore determined DCBs or inter-frequency biases of the test receivers. Knowledge of the DCBs is of particular relevance for ionospheric studies but difficult to obtain in actual space missions (Heise et al. 2004). The use of a GPS signal simulator applies the unique opportunity to generate signals without ionospheric path delays or to remove the respective contributions in the measurements using the known simulator models. Results of this analysis are summarized in Table 4, which shows particularly pronounced offsets for the IGOR receiver. Despite an obvious scatter among different units of the same receiver type as well as different data sets collected with the same receiver, the reported values may serve as a guideline for a future analysis of flight data.

Navigation accuracy

The navigation solution accuracy of the IGOR, OEM-4, and PolaRx2 receivers has been assessed over a 15-h data arc in comparison with the simulated reference trajectory. A vertical total electron content of $10 \text{ TECU} = 10^{17} \text{ e}^-/\text{m}^2$ (representative of a 500-km orbit at mean solar activity) was modeled, but no broadcast ephemeris errors were applied. The results demonstrate notable performance differences, which do not correspond to the underlying raw measurement accuracy. Instead, the navigation accuracy depends on specific

Table 4 Differential code biases (DCB). Unless otherwise specified, the biases exhibit a typical scatter of 0.1 m in different tests of the same receiver unit

Receiver	Unit	P1–C1 (m)	P2–C1 (m)	P2–P1 (m)
IGOR	a	+0.3	+4.7	+4.4
OEM4-G2	a		+2.3	
	b		+1.6 \pm 0.2	
PolaRx2	a	-0.3	0.0	+0.3
	b	-0.5	+0.1	+0.6
	c	-0.4	+0.1	+0.5

processing (single vs. dual frequency, data weighting, filtering, measurement corrections, etc.) employed in the receivers (Table 5).

The IGOR receiver performs a simple single-frequency navigation solution. This approach is considered to be most robust and maximizes the availability in case of weak signals, interference, and scintillation, but suffers from pronounced ionospheric errors. As a result, the navigation solution exhibits a mean radial position offset (Fig. 9) of about 0.8 m/TECU that is proportional to the vertical total electron content. The noise of the position solution amounts to roughly 3 m in radial and 1 m in along-track/cross-track direction, which is certainly more than would be expected from the very low C/A code measurement noise and the horizontal/vertical dilution of precision (HDOP \sim 1–2, VDOP=2–3). The OEM4-G2, in contrast, shows an unexpected negative bias of 14 m in the radial direction. It can best be attributed to the application of tropospheric delay corrections, which, of course, are meaningless for orbiting spacecraft. On the other hand, the solution accuracy is independent of the ionospheric path delays and must therefore be based on dual-frequency measurements. A superior position accuracy of roughly 1 m (3D) is finally demonstrated by the PolaRx2 receiver. The navigation solution is unbiased in all coordinates and exhibits a noise level that is even smaller than expected from the noise of the ionosphere-free pseudo-range combination ($\sigma_{P12} \approx 0.6$ m) and the position dilution of precision (PDOP \sim 3). Besides the use of dual-frequency measurements, the low noise of the navigation solution can be attributed to a signal-quality dependent data weighting along with a short-term Kalman-filtering inside the PolaRx2 receiver (J. Leyssens, private communication).

All receivers show a velocity accuracy of about 0.1 m/s, which relates to a Doppler accuracy of 2–4 cm/s. Biases may again be recognized for two receivers in the radial position component, albeit at the level of the data noise. Given a predominantly radial acceleration of a LEO satellite of magnitude $a \approx 8.5 \text{ m/s}^2$, these biases can be interpreted as timing offsets of the employed range-rate measurements. A 5-ms offset could indeed be identified in the Doppler measurements of the OEM4-G2 receiver. For the IGOR receiver, Doppler data are only internally available which prevents a further analysis.

POD performance

Complementary to the navigation solution accuracy, which is primarily of relevance for real-time and on-board applications, we assessed the precise orbit determination (POD) accuracy that can be achieved in postprocessing. To this end, 15-h data arcs were pro-

Table 5 Navigation solution accuracy in the presence of ionospheric path delays (VTEC = 10TECU) but excluding contributions due to ephemeris errors

Position (m)	Radial (m)	Along-track (m)	Cross-track (m)	Position (3D rms) (m)
IGOR	$+8.4 \pm 3.3$	$+0.4 \pm 1.3$	-0.0 ± 1.2	9.2
OEM4-G2	-13.9 ± 5.7	$+0.1 \pm 2.4$	$+0.1 \pm 2.1$	15.3
PolaRx2	-0.1 ± 1.0	$+0.0 \pm 0.5$	$+0.1 \pm 0.4$	1.2
Velocity	Radial (m/s)	Along-track (m/s)	Cross-track (m/s)	Velocity (3D rms) (m/s)
IGOR	$+0.09 \pm 0.07$	$+0.00 \pm 0.04$	-0.00 ± 0.03	0.12
OEM4-G2	-0.06 ± 0.05	-0.01 ± 0.03	-0.00 ± 0.02	0.08
PolaRx2	-0.01 ± 0.07	$+0.01 \pm 0.03$	$+0.00 \pm 0.03$	0.09

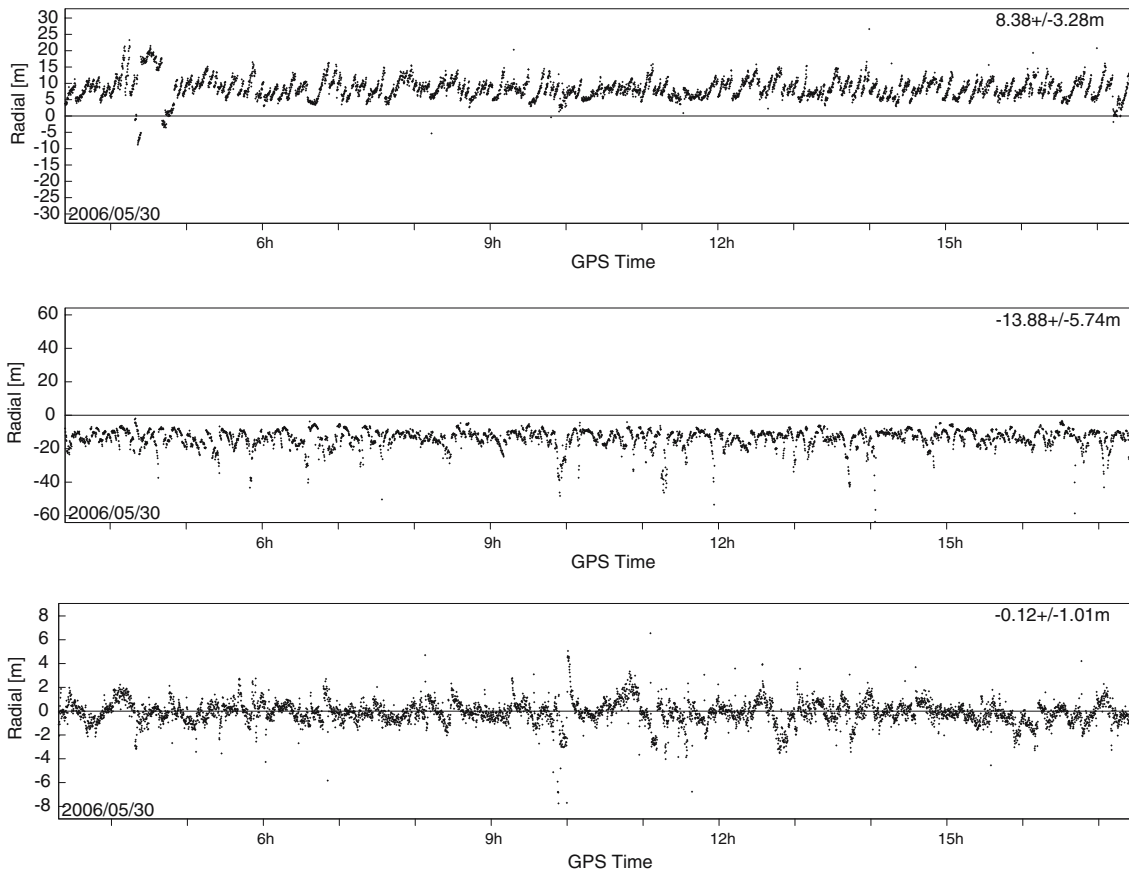


Fig. 9 Errors of the navigation solution (radial position component) computed by the IGOR (*top*), OEM4-G2 (*center*), and PolaRx2 (*bottom*) receivers in the presence of ionospheric path delays (VTEC = 10TECU) but excluding contributions due to ephemeris errors. Note the different scales

cessed with DLR's GHOST software for reduced dynamic orbit determination (Montenbruck et al. 2005). Results for different types of ionosphere-free measurements (P12 code, L12 carrier phase, and C/A code plus LA phase combination) are collated in Table 6. Despite the obvious differences in the raw data quality, the

three test receivers show surprisingly consistent orbit determination results with accuracies of typically 15–20 cm for dual-frequency code measurements, 3 cm for dual-frequency carrier phase measurements, and 10–15 cm for single-frequency code-carrier combinations. This consistency is partly driven by the high level of dynamical smoothing applied in the orbit determination process. On the other hand, differences between the simplifying dynamical models of the signal simulator and the real-world dynamics models employed in the orbit determination software may limit the achievable POD accuracy in these tests and overcast

Table 6 Precise orbit determination performance (residuals and position error) using different data combinations

Receiver	Data	Residuals (cm)	Radial (m)	Along-track (m)	Cross-track (m)	Position (3D rms) (m)
IGOR	P12	59	-0.02 ± 0.06	-0.01 ± 0.10	$+0.06 \pm 0.09$	0.16
	L12	0.5	-0.00 ± 0.01	-0.01 ± 0.01	$+0.01 \pm 0.01$	0.03
	C1 + LA	5.9	-0.02 ± 0.03	-0.05 ± 0.03	$+0.05 \pm 0.02$	0.09
OEM4-G2	P12	158	-0.04 ± 0.07	$+0.07 \pm 0.11$	$+0.02 \pm 0.08$	0.17
	L12	0.4	-0.00 ± 0.02	$+0.02 \pm 0.01$	$+0.01 \pm 0.01$	0.03
	C1 + LA	19	-0.02 ± 0.05	$+0.03 \pm 0.12$	$+0.06 \pm 0.05$	0.16
PolaRx2	P12	64	-0.03 ± 0.07	-0.04 ± 0.11	-0.00 ± 0.12	0.19
	L12	0.8	-0.00 ± 0.01	-0.01 ± 0.01	0.01 ± 0.01	0.03
	C1 + LA	9.7	-0.03 ± 0.03	-0.01 ± 0.05	0.06 ± 0.03	0.09

performance differences related to the raw data noise. Nevertheless, our results provide proper evidence that all three receivers are well suited for POD of low Earth satellites and encourage their use in actual space missions.

Summary and conclusions

A detailed comparison of three semicodeless GPS receivers has been performed to assess their suitability for space applications. It is demonstrated that high-quality dual-frequency measurements in LEO cannot only be obtained by a dedicated spaceborne GPS receiver (IGOR), but also with commercial-off-the-shelf receivers (OEM4-G2, PolaRx2) that have received little to no modifications for coping with the increased signal dynamics. All test receivers enable a robust cold start acquisition and provide accurate code and carrier phase measurements for POD and formation flying applications. The real-time navigation solution, in contrast, does not exploit the potential of the available raw measurements in case of the IGOR and OEM4-G2 receivers. Besides enhancements of the single-point navigation solution the provision of a Kalman filtered solution appears desirable for a better support of on-board navigation needs.

Among the three test receivers, the IGOR instrument is certainly best prepared for occultation measurements aiming at a restitution of tropospheric temperature and pressure profiles in view of its superior tracking sensitivity and the specially designed flight software. The OEM4-G2 receiver, in contrast, offers an extremely low power consumption which allows its use on even a picosatellite. The PolaRx2 receivers, finally, provide an ideal candidate for applications requiring low-noise measurements such as carrier phase differential navigation or ionospheric electron content measurements.

Even though extensive environmental tests and further qualification measures are deemed necessary for an actual space application, the use of COTS technology is expected to provide a viable alternative to fully space qualified receivers. Aside from expected cost benefits, it will help to improve development cycles and accelerate the mission readiness of emerging receiver technologies. This is of particular interest as a growing number of new navigation signals will be emitted by the Galileo constellation and the next generation GPS satellites. These will ultimately render semicodeless tracking techniques for encrypted P(Y)-code obsolete, which currently represent a major limitation for low-sensitivity and high accuracy dual-frequency tracking.

Due to the lack of access to dedicated spaceborne dual-frequency receivers developed by European and Japanese manufacturers (Lagrange, GRAS, DFSG, etc.) the present study is necessarily incomplete and provides only a partial picture of the achievable tracking and navigation performance in space. It is hoped, however, that the performed work triggers further research in this area and provides a thorough basis for comparison as soon as performance data for the aforementioned receivers becomes publicly available.

Acknowledgments Testing of the IGOR flight unit for the TerraSAR-X project has been enabled through the GeoForschungs-Zentrum, Potsdam, which also provided an engineering model of the CHAMP choke ring antenna for ground verification. Prof. E.G. Lightsey, Center for Space Research of the University of Texas at Austin, and Prof. Ch. Günther, Institute of Communications and Navigation of the German Aerospace Center (DLR), have kindly provided access to their Spirent GPS signal simulators. OEM4-G2 and PolaRx2 receivers with deactivated altitude and speed limitations have been provided by NovAtel, Canada, and Septentrio, Belgium, with permission of local governmental authorities. The authors gratefully acknowledge the support of all institutions and individuals, which have been vital for a successful performance of the present study.

References

- Ardaens J-S (2005) Experimental analysis of a choke ring antenna; DLR-GSOC TN 05-05. Deutsches Zentrum für Luft- und Raumfahrt, Oberpfaffenhofen
- BRE (2003) Integrated GPS occultation receiver IGOR; data sheet. Broadreach Engineering, Tempe, Arizona
- Buist P (2002) NEC/Toshiba Space Systems' spaceborne GPS receivers. In: Presented at NEC/Toshiba, December 2002, Yokohama
- Fenton PC, Petersen WD (1998) Dual frequency global positioning system. US Patent 5736961, April 7, 1998
- Gurtner W, Estey L (2002) RINEX Version 2.20—modifications to accommodate low earth orbiter data; April 15, 2002. URL http://ftp.unibe.ch/aiub/rinex/rnx_leo.txt
- Heise S, Stolle C, Schlüter S, Jakowski N (2004) Differential code bias of GPS receivers in low earth orbit: an assessment for CHAMP and SAC-C. In: Reigber CH, Lühr H, Schwintzer P, Wickert J (eds) CHAMP mission results for gravity and magnetic field mapping, and GPS atmosphere sounding. Springer, Berlin Heidelberg New York
- Kroes R, Montenbruck O, Bertiger W, Visser P (2005) Precise GRACE baseline determination using GPS. GPS Solutions 9:21–31 DOI 10.1007/s10291-004-0123-5
- Kursinski ER, Hajj GA, Hardy KR, Schofield JT, Linfield RP (1997) Observing Earth's atmosphere with radio occultation measurements using the global positioning system. J Geophys Res 102/D19:23429–23465
- Langley RB, Montenbruck O, Markgraf M, Kang CS, Kim D (2004) Qualification of a commercial dual-frequency GPS receiver for the e-POP platform onboard the Canadian CASSIOPE spacecraft. In: Second ESA workshop on satellite navigation user equipment technologies, NAVITEC'2004, December 8–10, 2004, Noordwijk, The Netherlands
- Lear WM (1987) GPS navigation for low-earth orbiting vehicles; NASA 87-FM-2, Rev. 1; JSC-32031, Lyndon B. Johnson Space Center, Houston
- Leyssens J, Markgraf M (2005) Evaluation of a commercial-off-the-shelf dual-frequency GPS receiver for use on LEO satellites. In: ION GNSS 2005 conference, September 13–16, 2005, Long Beach, California
- Markgraf M, Montenbruck O (2004) Total ionizing dose testing of the NovAtel OEM4-G2L GPS receiver; DLR-GSOC TN 04-04. Deutsches Zentrum für Luft- und Raumfahrt, Oberpfaffenhofen
- Marradi L, Banfi E, Mambretti A (2001) The Lagrange receiver: design and in-flight demonstration. NAVITECH'2001, December 10–12, 2001, Noordwijk
- Meehan TK, Thomas JB Jr, Young LE (2000) P-code enhanced method for processing encrypted GPS signals without knowledge of the encryption code. US Patent 6061390, May 9, 2000
- Montenbruck O, Holt G (2002) Spaceborne GPS receiver performance testing; DLR-GSOC TN 02-04. Deutsches Zentrum für Luft- und Raumfahrt, Oberpfaffenhofen
- Montenbruck O, Kroes R (2003) In-flight performance analysis of the CHAMP BlackJack receiver. GPS Solut 7:74–86
- Montenbruck O, van Helleputte T, Kroes R, Gill E (2005) Reduced dynamic orbit determination using GPS code and carrier measurements. Aerospace Sci Technol 9/3:261–271 DOI 10.1016/j.ast.2005.01.003
- Rankin D, Kekez DD, Zee RE, Pranajaya FM, Foisy DG, Beattie AM (2004) The CanX-2 nanosatellite: expanding the science abilities of nanosatellites. In: Proceedings of the 55th International Astronautical Congress, October 2004, Vancouver, Canada
- Reigber CH, Jochmann H, Wunsch J, Petrovic S, Schwintzer P, Barthelmes F, Neumayer K-H, König R, Förste CH, Balmino G, Biancale R, Lemoine J-M, Loyer S, Perosanz F (2004) Earth gravity field and seasonal variability from CHAMP. In: Reigber CH, Lühr H, Schwintzer P, Wickert J (eds) Earth observation with CHAMP—results from three years in orbit. Springer, Berlin Heidelberg New York, pp 25–30
- Silvestrin P, Cooper J (2000) Method of processing of signals of a satellite positioning system. US Patent 6157341, December 5, 2000
- Silvestrin P, Bagge R, Bonnedal M, Carlström A, Christensen J, Hägg M, Lindgren T, Zangerl F (2000) Spaceborne GNSS radio occultation instrumentation for operational applications. In: ION-GPS-2000 conference, Salt Lake City, September 19–22, 2000, pp 872–880
- Spirent (2004) SimGEN (including SimLocate) user manual—software for the Spirent range of satellite navigation simulator products; DGP00686AAA; Issue 1–13, August 2004
- Thomas JB (1995) Signal-processing theory for the TurboRogue receiver. JPL Publication 95–6, April 1, 1995
- Van Dierendonck AJ (1995) GPS receivers. In: Spilker J, Parkinson B (eds) Global positioning system: theory and applications, vol I, chapt. 8. American Institute of Aeronautics and Astronautics Inc., Washington
- Williams J, Lightsey EG, Yoon SP, Schutz RE (2002) Testing of the ICESat BlackJack GPS receiver engineering model. In: ION-GPS-2002 conference, September 24–27, 2002, Portland, Oregon
- Woo KT (2000) Optimum semi-codeless carrier phase tracking of L2. Navigation: J Inst Navigation 47(2):82
- Wu B-H, Chu V, Chen P, Ting TH (2005) FORMOSAT-3/COSMIC science mission update. GPS Solut 9:111–121
- Yunck TP (2004) Spaceborne GPS for POD and earth science. In: Reigber CH, Lühr H, Schwintzer P, Wickert J (eds) Earth observation with CHAMP—results from three years in orbit. Springer, Berlin Heidelberg New York, pp 25–30